NASA Technical Memorandum 79066

EXPERIMENTAL EVALUATION OF THE EFFECT OF INLET DISTORTION ON COMPRESSOR BLADE VIBRATIONS

J. F. Lubomski
Lewis Research Center
Cleveland, Ohio

TECHNICAL PAPER to be presented at the
International Gas Turbine Conference
sponsored by the American Society of Mechanical Engineers
San Diego, California, March 12-15, 1979

EXPERIMENTAL EVALUATION OF THE EFFECT OF INLET DISTORTION ON COMPRESSOR BLADE VIBRATIONS

J. F. Lubomski
Aerospace Research Engineer
National Aeronautics and Space Administration
Lewis Research Center
Cleveland, Ohio

E-9882

ABSTRACT

Compressor rotor strain gage data from an engine test conducted with an inlet screen distortion were reduced and analyzed. These data are compared to data obtained from the same engine without inlet pressure distortion to determine the net effect of the distortion on the vibratory response of the compressor blades. The results obtained are presented.

INTRODUCTION

Inlet distortion, besides seriously affecting fan and compressor stall margin and performance, can also generate blade and vane vibrations that can significantly affect the structural integrity of the blades and vanes. Although this has been known to fan and compressor designers for a number of years, it has only been recently comprehensively treated (Refs. 1 and 2).

NASA has been actively involved with engine research relative to inlet distortion for a number of years. This involvement was primarily concerned with the effects of inlet distortion on engine performance and stall margin. It has been only recently that the structural dynamic aspects of the problem have been considered. The impetus for this interest has been generated by the aeromechanical programs within the NASA/USAF Full Scale Engine Research (FSER) Program. Extensive strain gage monitoring and other dynamic data acquisition and reduction systems have been incorporated into existing engine test facilities used in the FSER programs to support the aeromechanical programs. These systems are now available and are being used in support of research related to inlet distortion. They were first used for this purpose recently to monitor a series of inlet pressure distortion tests being conducted on an engine. This particular engine had been previously used in an aeromechanical program and still had a number of meaningful strain gages operational. Data from these were monitored and recorded to observe the effects of inlet pressure distortion on the structural response of the compressor blades. During the test no serious problems were observed and all stress levels stayed well within limits. It was only after doing a Fourier Analysis of the recorded data was the data found to be significant. In particular, when comparing data with and without inlet distortion the data revealed the elements necessary for serious compressor blade vibrations to develop with inlet distortion.

The purpose of this paper, then, is to describe the test conditions, the methods used in obtaining and reducing these data, and to discuss the significance of it.

NOMENCLATURE

E	engine order
f	frequency
I	impulse function
P	pressure
r	cylindrical coordinate

t time
x displacement amplitude
θ cylinderidal coordinate
φ phase angle

Subscripts:

n integer
T total
2 station 2, engine inlet

APPARATUS AND TEST CONDITIONS

The test vehicle used was a straight turbojet engine with a nine-stage compressor (Fig. 1), the first two of which have part span shrouds. The first three stator stages are variable. These were rigged in the nominal operational configuration for the distortion tests. This configuration was found to be safe from any severe resonances or aeroelastic instability within the flight envelope of this engine during the aeromechanical test phase. The distortion tests were conducted in the Propulsion System Laboratory Altitude Facility at the NASA Lewis Research Center. A variety of inlet distortion screens were used, all of which produced a one-engine order (1E) stimulus but of different intensities and distribution.

As a rule the majority of engine inlet distortion testing conducted at Lewis is done with an inlet pressure of 0.5 atmospheres and inlet temperatures around 15.6° C (60° F). These altitude conditions are considered safe relative to structural considerations. At these conditions resonance responses are normally mild, aeroelastic instabilities are rare and blade loading is moderate. The latter is desirable if a number of compressor stalls are to be induced which is usually the case in distortion testing. The availability of operational strain gages presented the opportunity to obtain data at more severe operating conditions to evaluate the structural dynamic aspects of inlet pressure distortions. The inlet pressure distortion data to be discussed herein was obtained at an inlet pressure of 138 kPa (20 psia) and at an inlet temperature of 15.6° C (60° F). These were the most severe conditions used and are representative of a high-speed flight condition at a low altitude on a cold day. These flight conditions produce heavy blade loading with dense air. A data run consisted of an intermittent slow acceleration of the engine from 90 to 104.5% rated physical speed. All speeds discussed herein shall be rated engine physical speeds. The acceleration was halted several times to take steady-state aerodynamic data. Strain gages were monitored and recorded during the entire period.

The inlet screen used is shown in Fig. 2. This screen imposes a circumferential pressure distortion over a full 180° sector of the engine inlet with an aggravated radial distortion centered within that sector at the outside diameter. The pressure distortion pattern generated by this screen produces a 1E stimulus which is representative of a maneuvering distortion. Inlet total pressure distribution patterns obtained from aerodynamic data are shown in Figs. 3 and 4. The data in Fig. 3 was obtained ad 95% speed while the data in Fig. 4 was at 104% speed. At 95% the minimum $\Delta P/\overline{P}$ was -0.080 and at 104% - 0.120. $\Delta P/\overline{P}$ is a distortion index defined as:

$$P_{T2}(r,\theta) - P_{T2}(\text{AVERAGE})/P_{T2}(\text{AVERAGE})$$

where $P_{T2}(r,\theta)$ is the station 2 total pressure at a point, and $P_{T2}(\text{AVERAGE})$ is the station 2 average total pressure.

For comparative clean inlet strain gage data, transient data from a previous aeromechanical data point was reduced. This data point was obtained with inlet conditions of 200 kPa (20 psia) and 15.6° C (60° F). This data point was selected because it had the same variable geometry rigging, was free of aeroelastic instabilities and was the best match of the conditions available with a clean inlet. The data in this transient was obtained while doing a slow acceleration from 97 to 104.5% rated physical speed.

DYNAMIC DATA ACQUISITION

Structural dynamic data pertinent to the blades and vanes in an engine under test is gathered from three sources in the Propulsion Systems Laboratory Facility at Lewis. These are:

(1) Strain gage systems, rotating and stationary.
(2) Photo-electric scanning (PES) system.
(3) High response pressure transducers.

Strain gages mounted on blades and vanes are the primary source of structural dynamic data. The other two systems were not used in this analysis but are described in Refs. 3 and 4. The strain gages are monitored on line, in real time during a test, in both the time domain and in the frequency domain. Each strain gage signal is displayed on a small oscilloscope for continuous monitoring in the time domain. Up to 112 signals can be handled simultaneously using this approach. In addition, these signals can be quickly patched into large oscilloscopes for a more comprehensive analysis in the time domain. These signals can also be quickly and selectively patched into other equipment for monitoring and analysis in the frequency domain. This equipment includes:

(1) A software based Fast Fourier Transform (FFT) Digital Signal Analyzer which can handle two channels simultaneously.
(2) Several analog spectral analyzers.
(3) A micro-processor based multi-channel vibration and flutter monitor (Ref. 5) which can handle up to 16 channels simultaneously.

All strain gage data is recorded for post run analysis. Within the test facility up to 40 channels are available on a local recording system. Strain gage data is also transmitted via underground lines to a Central Analog System which has 180 channels available for data recording.

During the inlet pressure distortion tests the principle source of structural dynamic data were the strain gages since the engine had more than adequate strain gage coverage on all pertinent compressor rotors except one. The fourth stage rotor had lost all of its gages, therefore, the PES system was used to monitor this stage for safety purposes.

DYNAMIC DATA REDUCTION

The majority of the dynamic data obtained to date has been recorded in analog form. Data reduction thus is done both in the time domain and in the frequency domain by use of the Fourier Transform. Time domain data reduction yields wave form information and the overall magnitude of the signal. Frequency domain data reduction is useful in mode indentification, in determining multiple mode responses, in determining engine order content and in determining the amplitudes of all the contributing harmonics. Time domain data reduction is primarily done using conventional cathode ray oscillographs to determine wave form and amplitude. Frequency domain data reduction is done by using several FFT systems and by digitizing analog data and using an FFT algorithm routine available on a main frame computer. In the frequency domain the data are processed to obtain power spectral density, linear spectra, transfer function, and cross-correlation function. The latter two yield both magnitude and phase as functions of frequency. Time averaging is used frequently and when this is done the coherence function is also computed. Data output is in the form of computer printouts and plots. As a practice frequency resolution is usually of the order of 1 Hz. Phase angle data obtained is accurate well within 1^{o}.

The data discussed herein were reduced from local tapes in the test facility. All the data were observed in the time domain and in the frequency domain to determine which data were of significance. The data of significance were then processed through the FFT Digital Signal Analyzer.

RESULTS AND DISCUSSION

Based on preliminary data reduction and analysis a number of strain gages from the first three compressor rotor stages were selected for detailed analysis. Strain gage locations on the compressor blades are shown in Fig. 5. Rotors 1 and 2 were selected because the strain gages on these showed the largest increase in vibratory response compared to clean inlet data. With a clean inlet both of these stages had a very low vibratory response. With the pressure distortion the vibratory response of the compressor blades increased but stayed well within allowable stress limits. At 94% speed and 138 kPa (20 psia) inlet pressure the first rotor was showing about ±21 MPa (±3 ksi) in the time domain. The only sizeable activity usually observed on the second rotor with a clean inlet occurred in above the shroud first torsion at 7E around 95% speed. At elevated inlet temperatures the overall vibratory response was higher, usually of the order of about ±28 MPa (±4 ksi) in the time domain. Other than this the second rotor was well behaved. With the distortion the overall response of the second rotor increased by about a factor of 2. Rotor 3 was selected because it has the most active resonance response with a clean inlet. At speeds in excess of 100% rated physical first bending would come in at 2E with overall stress levels of ±34.5 MPa (±5 ksi). With a distorted inlet the overall third rotor response was only slightly higher. The remaining stages showed no perceptible increase in strain gage response with a distorted inlet when compared to clean inlet data.

The data processed through the FFT Digital Signal Processor was time averaged, eight averages, over the range from 0 to 4096 Hz which encompassed all of the activity noted during the initial data reduction. A number of data points were taken. Some of the results are tabulated in Tables I, II, and III. The amplitudes in these tables were corrected to account for strain gage sensitivity. Strain gage sensitivity related the stress (strain) at the gage location to the maximum stress in any vibratory mode, thus the data in the tables reflects the apparent maximum vibratory stress in any mode. The uncorrected data taken from the Digital Signal Processor is shown in Figs. 6 through 18. Looking at this data for each of the first three rotors proved to be enlightening with respect to the effect of an inlet distortion on blade vibrations.

The first stage rotor data was most significant. Without distortion the typical frequency domain response of a strain gage on rotor 1 is shown in Fig. 6. Inherent in all the data analyzed were two standing components of frequency. One was around 150 Hz and the other slightly above 500 Hz. These were in the playback system. Thus the only significant data in Fig. 6 occurs around 800 Hz and is of a trivial amplitude. Therefore, with a clean inlet rotor 1 over the speed range between 97 and 104.5% was found to be very well behaved. From monitoring observations this was found to be true for all speeds and conditions within the engine operating range. The only activity ever noted on rotor 1 occurred during the transient from startup to idle when first bending would appear for a short time. With distortion the response in the frequency domain is shown in Fig. 7, 94% speed, and in Fig. 8, 104% speed. Of significance here is the presence in the spectrum of almost all the engine orders in the frequency range analyzed. At 94% speed this effect is more pronounced. At this speed and condition several modes are being excited. Without distortion only a slight excitation of first bending was observed, while with distortion both the first and second system modes are responding as well as first bending, first torsion, and third bending. Also present is the 1E component which is to be expected due to the nature of the induced distortion. As engine speed was increased above 94% the overall amplitude of the strain gages on rotor 1 decreased. This is reflected

in the spectrum taken at 104% (Fig. 8). Still present are indications that almost every engine order is affecting the blade but at this speed coincidence between the engine orders and a blade or system resonance does not exist. The 1E component is still present and at about the same magnitude as was seen at 94% speed even though the distortion index is considerably more severe.

Apparent from this data is the fact that this stage is well damped at the inlet conditions set. Also apparent is the fact that the distortion being created by the 1E screen has the qualities of a complex harmonic wave, square wave, which is creating the numerous engine order excitations. This wave will have a period of 60/RPM (1/E) and in essence is composed of a number (N) sinusoids of various amplitude (An) and phases (φ_n or φ). In the time domain this wave is defined by:

$$x(t) = \sum_{n=1}^{N} A_n \cos(2\pi f_n + \varphi_n) \qquad f_n = \frac{n(RPM)}{60}$$

In the frequency domain this wave transforms to (Ref. 6)

$$X(f) = \sum_{n=1}^{N} \frac{1}{2} A_n \left[I(f - f_n) e^{j\varphi_n} + I(f + f_n) e^{-j\varphi_n} \right]$$

which when plotted for sequential values of N yields a spectrum plot similar to those being observed in the distortion data. Thus the data reveals the nature of the excitation that can be expected with an inlet pressure distortion. The rotor blade will see the pressure distortion as a periodic complex wave containing a number of multiples of the rotational frequency. Engine speed determines the period of the complex wave and the spacing of the successive harmonics in the frequency domain. Whenever any of the harmonics contained in the pressure distortion coincides with a blade or system resonance a response will occur. The magnitude of the response will be a function of the strength of distortion and the damping present in the aerodynamic mode. Of particular importance is the aerodynamic damping. The distortions induced during this test were severe, yet the first rotor response, while discernible, was not severe.

Rotor 2 data is shown in Table II and Figs. 9 through 12. Without pressure distortion at speeds under 95% the only notable response observed, on line, was a slight resonance affecting first torsion at 7E. Above 95% speed the rotor 2 response was slight and a typical spectrum is shown in Fig. 9. Present here is a slight response in first bending at 3E with a trace of the first two system modes. Also present is evidence of a slight internal distortion probably resulting from the interaction of the second rotor and first stator. With inlet pressure distortion the 1E response increased, as seen in Figs. 10 through 12, as did the second system mode. The 10E response could not be associated with a particular blade alone mode being between first torsion and second bending so it is assumed that the third system was also excited. The most activity on this stage occurred at 98% speed, Fig. 9, where coincidence between several modes and excitation sources occurred much like that observed on rotor 1 at 94% speed. The rotor 2 response to first torsion around 94% speed at 7E was not unusual since it commonly occurred there without distortion and did not appear to be aggravated by the distortion.

Rotor 3 data is shown in Table III and in Figs. 11 through 16 for two different strain gages. Strain gage No. 9 was located near the root at midchord and was primarily responsive to the bending modes. Strain gage No. 14 was located at the trailing edge and was responsive to both bending and torsional modes. This rotor had the most active resonant response without distortion. Above 100% speed first bending would respond at 2E with amplitudes between ±21 and ±28 MPa (±3 and ±4 ksi). Of interest on this rotor was whether or not an inlet distortion would aggravate this response and it did not. The maximum amplitude of this response occurred usually about 104% speed and an examination of the data in Table III and the figures indicate that if anything, the response may have been attenuated. This may be due to a density effect since the inlet pressures did differ. However, an increase in the 1E component was noted as well as some activity in first torsion with the distorted inlet. Absent in the third rotor data was a well-defined resonance coincidence as seen on rotors 1 and 2. It may be that none existed over the speed range investigated or that the effects of the higher harmonics were starting to be attenuated.

The remaining stages had no interesting data. Rotor 4 did not have a valid strain gage so it was monitored using the PES system. The only activity noted on this rotor occurred at 104% speed and consisted of a low amplitude, ±0.05 mm (±2 mils), non-integral blade response which may have been buffeting as a result of the distortion. This amplitude is equivalent to a stress of about ±1.4 MPa (±0.2 ksi). Rotors 5 and 6 showed only a slight 1E response and otherwise did not differ from the clean inlet response. It appears that the effect of the inlet pressure distortion was attenuated in the back stages of the compressor.

The prominent feature of the inlet distortion stimulus is the complex nature of the pressure wave developed which must be assumed to contain excitation sources at almost all engine orders. Thus, any mode if not properly damped, could be excited including some of the usually quiet higher modes. Of additional interest was the fact that the first two stages were sensitive to system mode excitations. Both of these stages are shrouded thus all the blades on each stage are mechanically coupled. This could lead to the possibility of encountering a system mode instability such as the type discussed by Carta (Ref. 7) if the aerodynamic conditions were adverse.

SUMMARY OF RESULTS

Compressor rotor strain gage data from an engine undergoing an inlet pressure distortion was reduced and analyzed. The results were compared to similar data obtained from the same engine with a clean inlet to determine the effect of the distortion on the vibratory response of the compressor blading. The distortion was principally a 1E circumferential type.

The effect of the distortion was found to be most prominent in the first three compressor stages. An increase in blade vibratory response was noted due to both a 1E stimulus and also because of the complex nature of the pressure front created by the flow around and through the screen. It was found that the rotating blades see the pressure distribution as a periodic complex harmonic wave composed of almost all engine order excitations. Rotor speed establishes the period of the complex wave and thus the frequencies of all the higher engine order excitations.

At certain speeds it was found that the complex pressure wave had the frequency content to excite a number of modes simultaneously. However, the overall magnitudes were small and well within allowable stress limits.

REFERENCES

1. Danforth, C. E., "Distortion Induced Vibration in Fan and Compressor Blades," AIAA Paper No. 74-232, Jan. 1974.
2. "Distortion Induced Engine Instability," ARARD Lecture Series No. 72, Advisory Group for Aerospace Research and Development, Paris, France, Oct. 1974.
3. Nieberding, W. C., and Pollack, J. L., "Optional Detection of Blade Flutter," ASME Paper No. 77-GT-66, Mar. 1977.
4. Kurkov, A., and Dicus, J., "Synthesis of Blade Flutter Vibratory Patterns Using Stationary Transducers," ASME Paper No. 78-GT-160, Apr. 1978.
5. Smalley, R. R., "Microprocessor - Based Multichannel Flutter Monitor Using Dynamic Strain Gage Signals," NASA TM X-71884, 1976.
6. Otnes, R. K., and Enochson, L., "Digital Time Series Analysis," Wiley, New York, 1972, pp. 15-16.
7. Carta, F. O., "Coupled Blade-Disk-Shroud Flutter Instabilities in Turbojet Engine Rotors," ASME Paper No. 66-WA/GT-6, Nov. 1966.

TABLE I. - FIRST ROTOR VIBRATORY RESPONSE IN THE FREQUENCY DOMAIN

Engine order	Mode	Without inlet pressure distortion	With inlet pressure distortion	
		104% speed	94% speed	104% speed
1E	----------	----------	± 2.1 MPa (± 0.3 ksi)	± 1.7 MPa (± 0.25 ksi)
2E	1st system (570 - 740 Hz)	----------	± 6.9 MPa (± 1.0 ksi)	± 4.1 MPa (± 0.6 ksi)
3E	1st bending (750 - 950 Hz)	± 3.4 MPa (± 0.5 ksi)	± 4.3 MPa (± 0.6 ksi)	Trace
5E	2nd system (1080 - 1330 Hz)	Trace	± 8.27 MPa (± 1.2 ksi)	------
8E	1st torsion (1960 - 2100 Hz)	----------	± 15.2 MPa (± 2.2 ksi)	------
15E	3rd bending (3660 - 4180 Hz)	----------	± 9.0 MPa (± 1.3 ksi)	------

TABLE II. - SECOND ROTOR VIBRATORY RESPONSE IN THE FREQUENCY DOMAIN

Engine	Mode	Without inlet pressure distortion	With inlet pressure distortion		
		104% speed	94% speed	98% speed	104% speed
1E	----------	Trace	± 4.1 MPa (± 0.6 ksi)	± 2.8 MPa (± 0.4 ksi)	± 4.1 MPa (± 0.6 ksi
2E	1st system (680 - 850 Hz)	Trace	± 2.1 MPa (± 0.3 ksi)	± 2.1 MPa (± 0.3 ksi)	± 3.1 MPa (± 0.45 ksi)
3E	1st bending (750 - 950 Hz)	± 15.5 MPa (± 2.25 ksi)	± 9.3 MPa (± 1.35 ksi)	± 15.5 MPa (± 2.25 ksi)	± 20.7 MPa (± 3.0 ksi)
5E	2nd system (1370 - 1630 Hz)	Trace	----------	± 4.8 MPa (± 0.7 ksi)	± 5.5 MPa (± 0.8 ksi)
6E-7E	1st torsion (1700 - 2000 Hz)	----------	± 24.0 MPa (± 3.5 ksi) @7E	± 21.0 MPa (± 3.0 ksi) @6E	----------

TABLE III. - THIRD ROTOR VIBRATORY RESPONSE IN THE FREQUENCY DOMAIN

Engine order	Mode	Without inlet pressure distortion	With inlet pressure distortion	
		104% speed	94% speed	104% speed
	Strain Gage No. 9			
1E	----------	Trace	± 4.8 MPa (± 0.7 ksi)	± 7.6 MPa (± 1.1 ksi)
2E	1st bending (500 - 600 Hz)	± 24.8 MPa (± 3.6 ksi)	± 10.3 MPa (± 1.5 ksi)	± 20.7 MPa (± 3.0 ksi)
4E	2nd bending (1100 - 1300 Hz)	± 4.8 MPa (± 0.7 ksi)	± 6.2 MPa (± 0.9 ksi)	± 4.8 MPa (± 0.7 ksi)
8E	1st torsion (2150 - 2250 Hz)	----------	± 10.3*MPa (± 1.5 ksi) *Uncorrected	----------
	Strain Gage No. 14			
1E	----------	Trace	± 6.6 MPa (± 0.95 ksi)	± 4.1 MPa (± 0.6 ksi)
2E	1st bending (500 - 600 Hz)	± 12.4 MPa (± 1.8 ksi)	± 8.3 MPa (± 1.2 ksi)	± 4.8 MPa (± 0.7 ksi)
8E	1st torsion (2150 - 2250 Hz)	± 2.8 MPa (± 0.4 ksi)	± 12.4 MPa (± 1.8 ksi)	± 11.0 MPa (± 1.6 ksi)

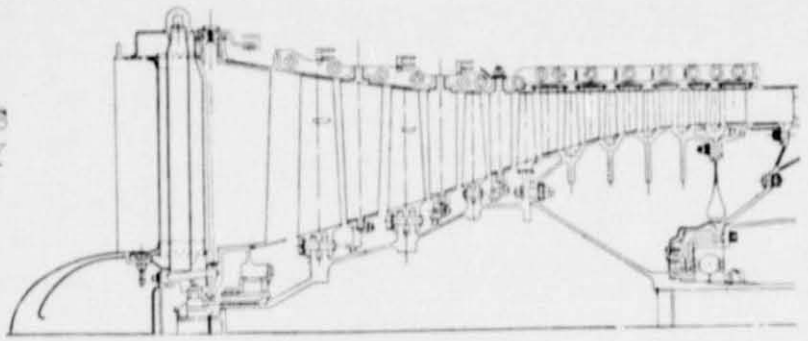

Figure 1. - Compressor cross section.

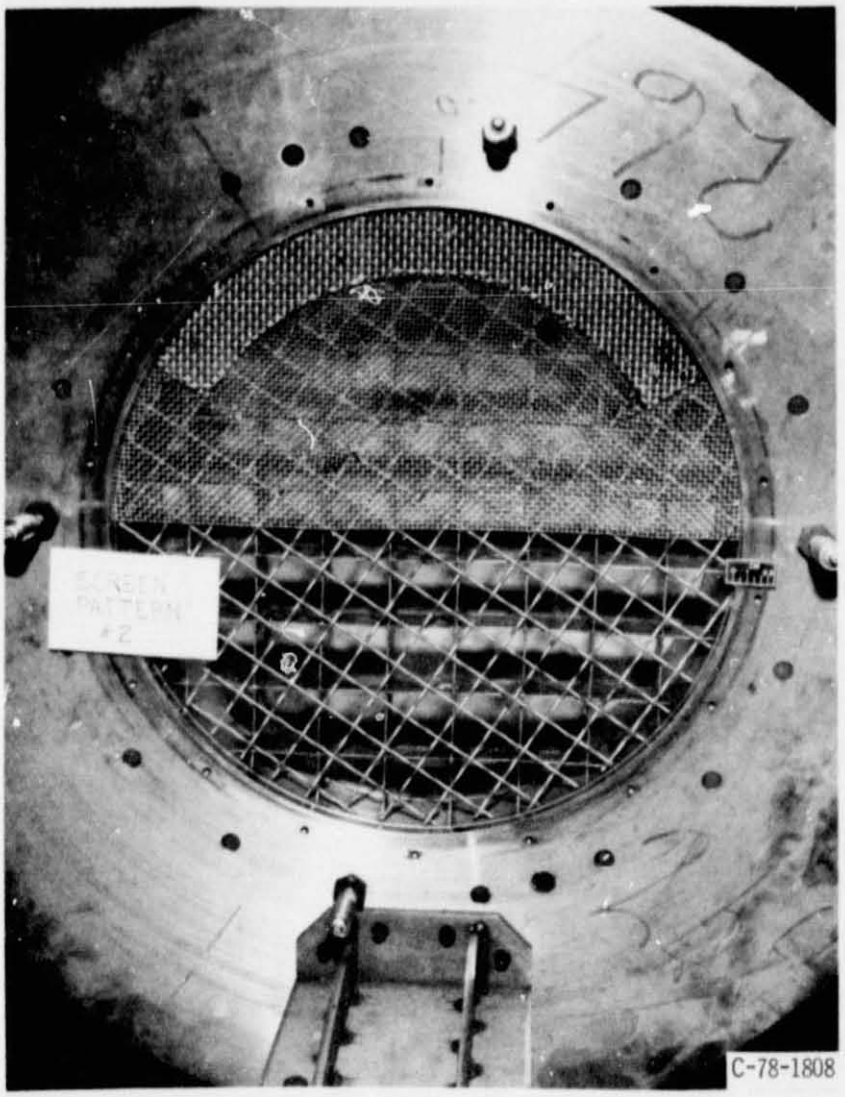

Figure 2. - Inlet distortion screen.

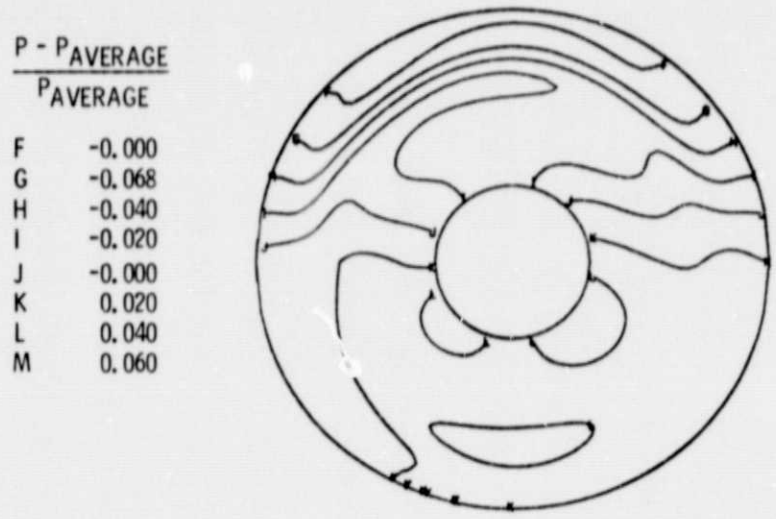

Figure 3. - Inlet total pressure distortion pattern at 95 percent physical speed.

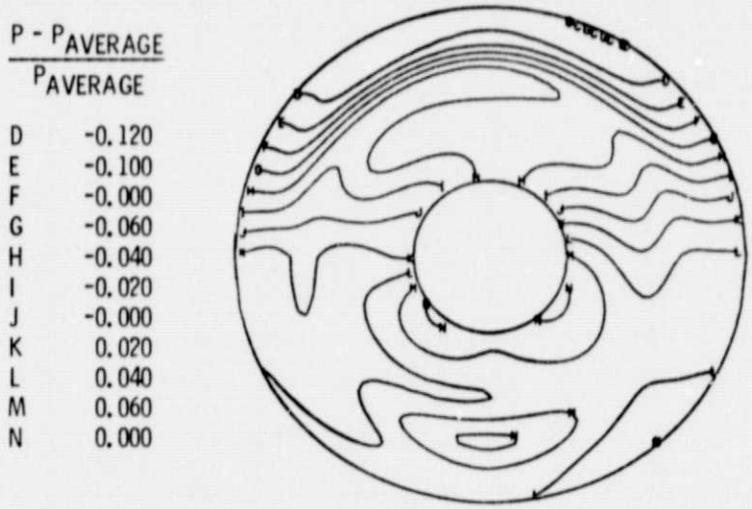

Figure 4. - Inlet total pressure distortion pattern at 104 percent physical speed.

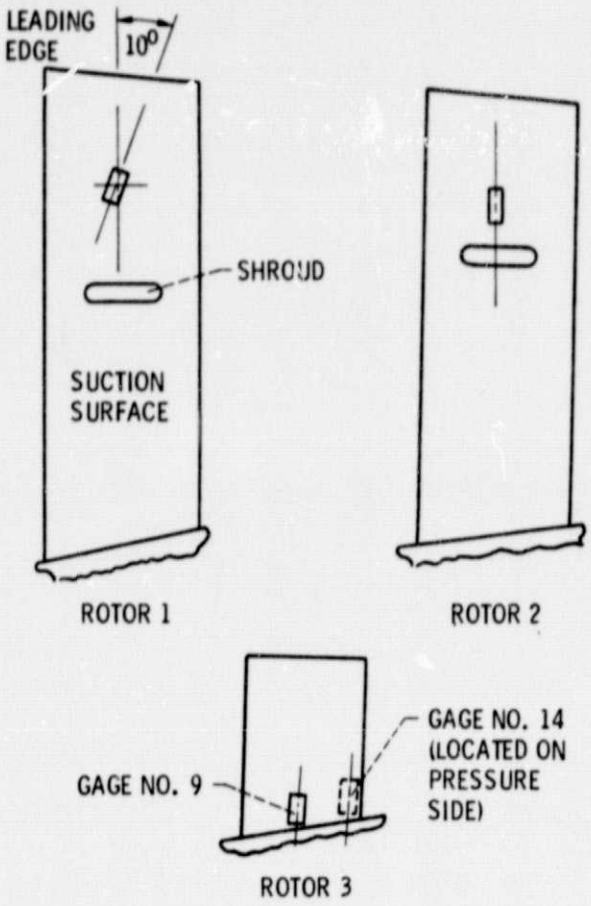

Figure 5. - Strain gage locations on rotor blades.

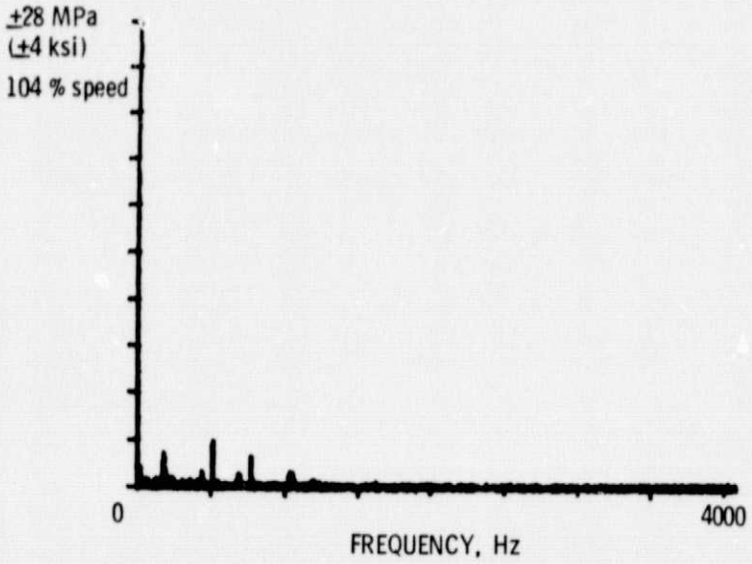

Figure 6. - Rotor 1 strain gage w/o screen.

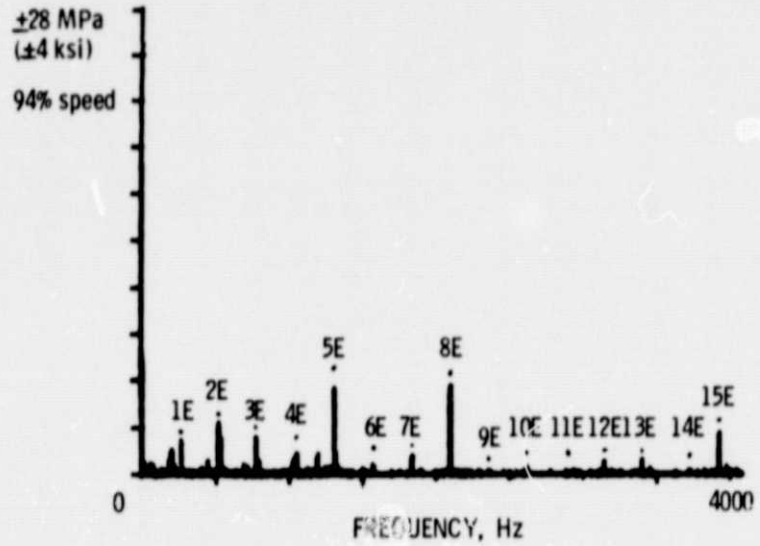

Figure 7. - Rotor 1 strain gage with distortion screen installed.

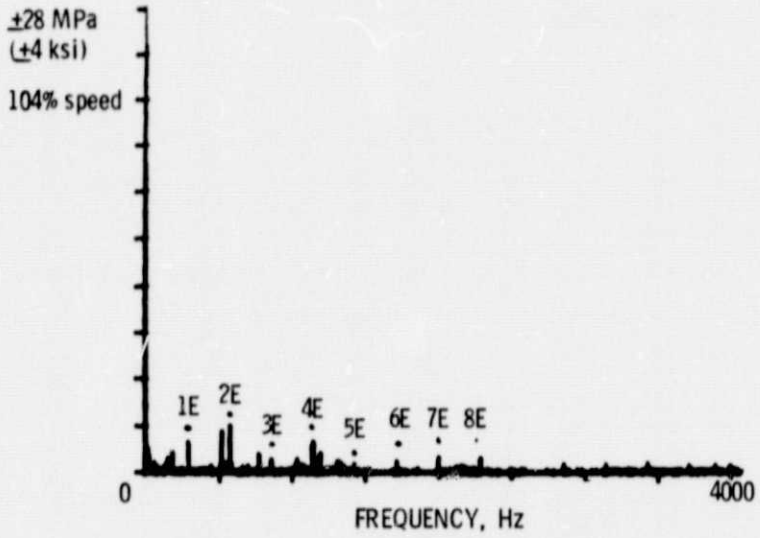

Figure 8. - Rotor 1 strain gage with distortion screen installed.

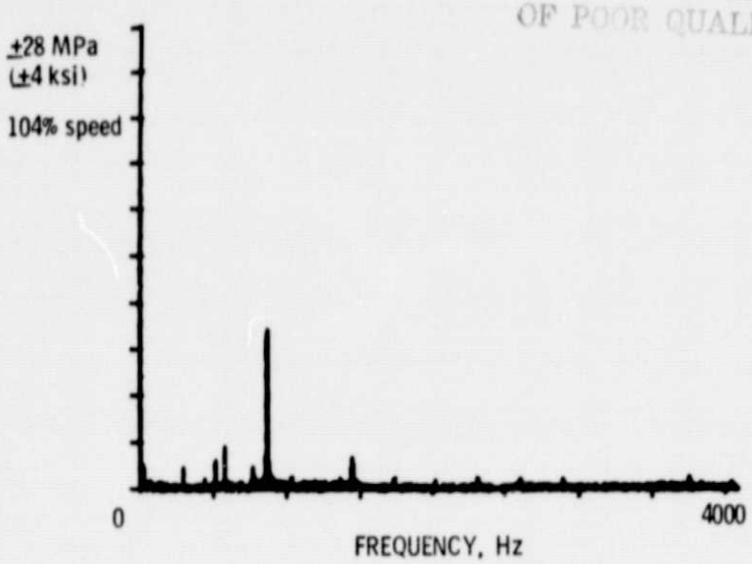

Figure 9. - Rotor 2 strain gage w/o screen.

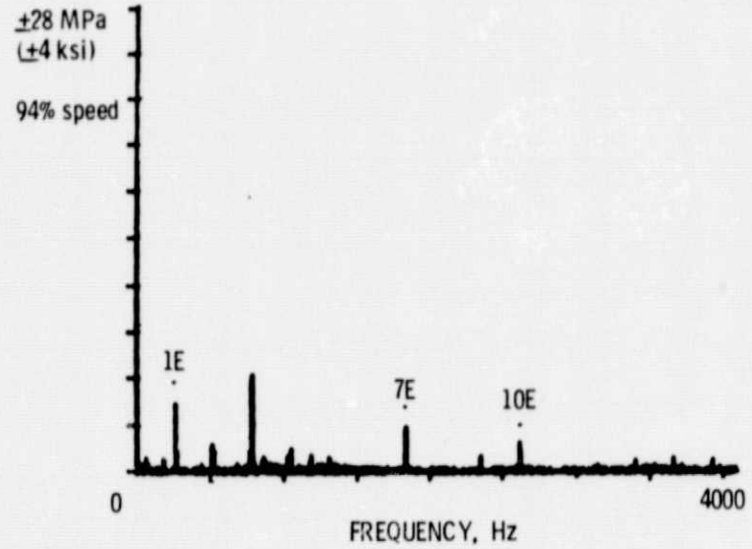

Figure 10. - Rotor 2 strain gage with distortion screen installed.

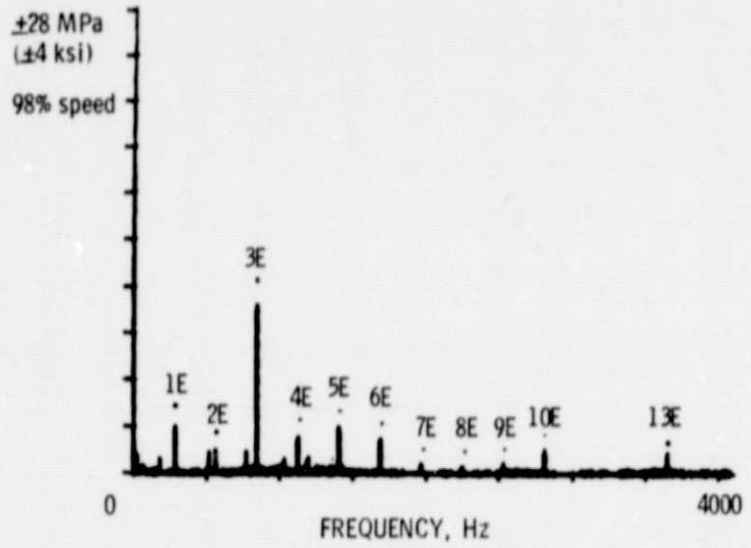

Figure 11. - Rotor 2 strain gage with distortion screen installed.

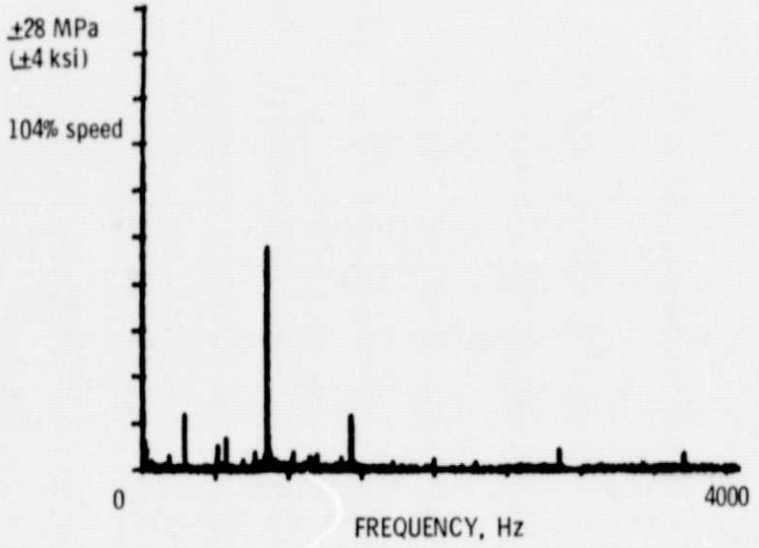

Figure 12. - Rotor 2 strain gage with distortion screen installed.

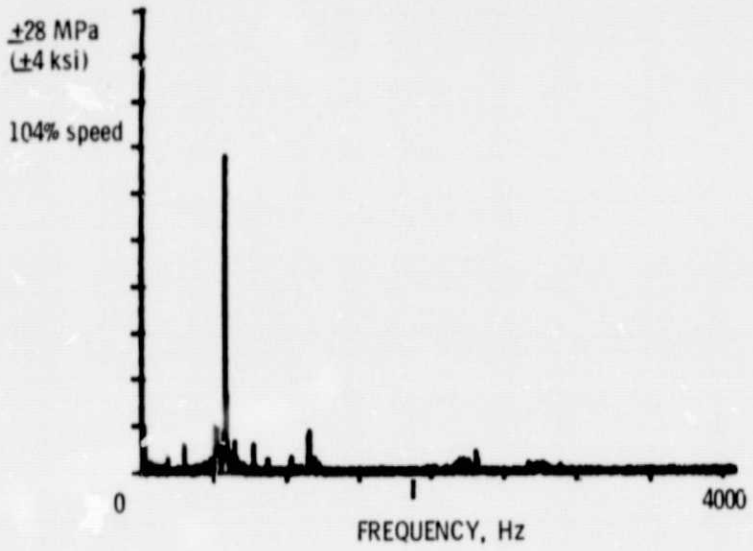

Figure 13. - Rotor 3, strain gage no. 9, without screen.

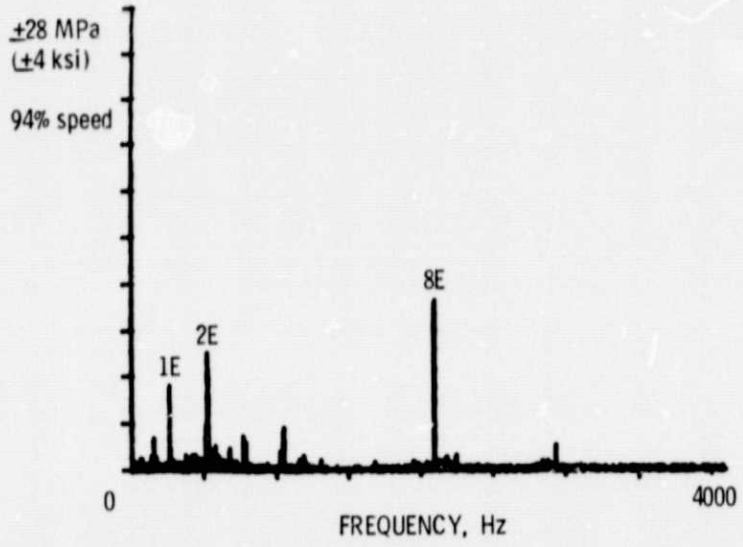

Figure 14. - Rotor 3, strain gage no. 9, with distortion screen.

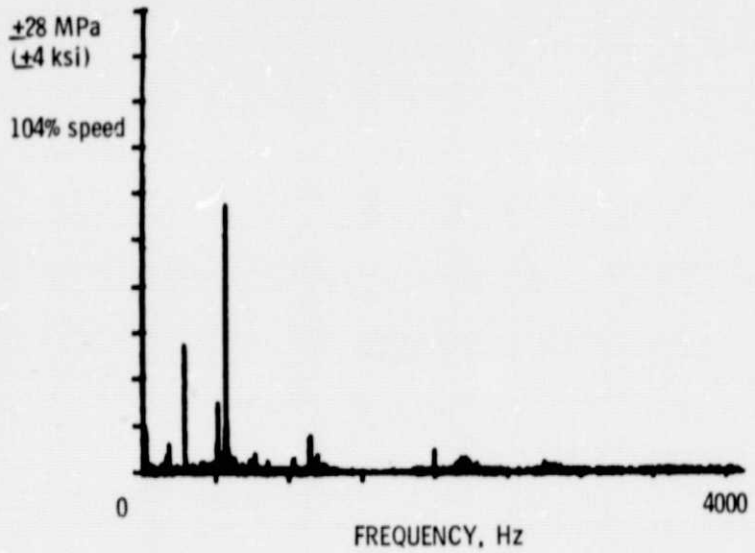

Figure 15. - Rotor 3, strain gage no. 9, with distortion screen.

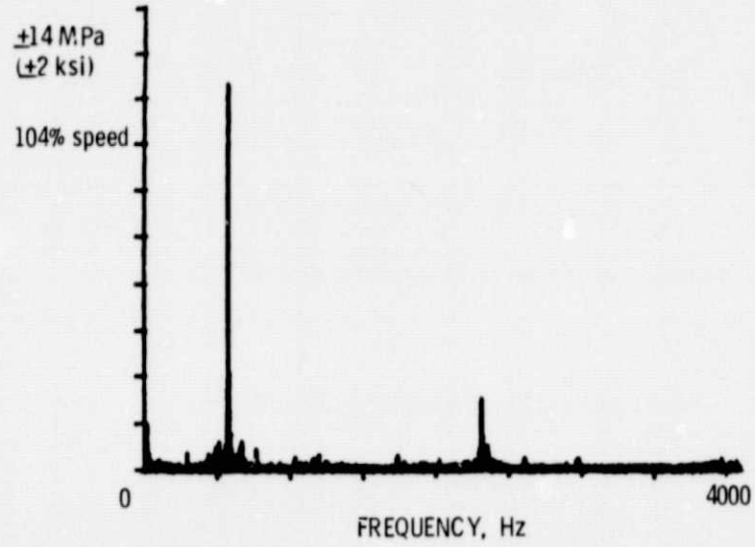

Figure 16. - Rotor 3, strain gage no. 14, without screen.

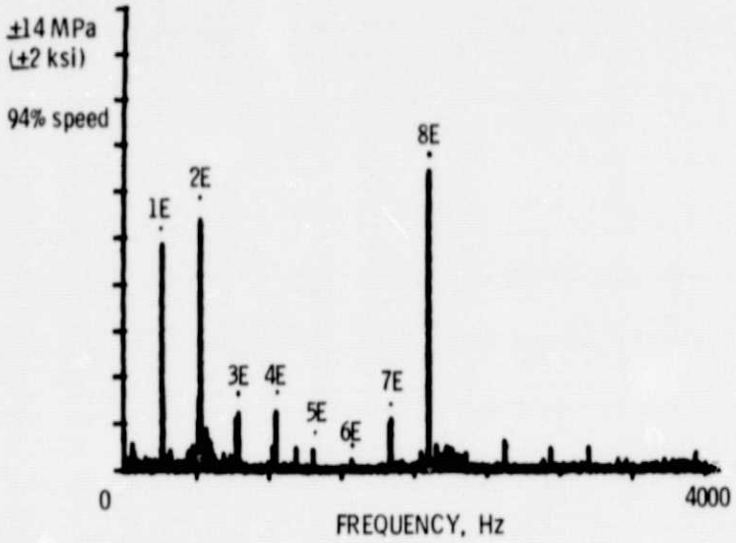

Figure 17. - Rotor 3, strain gage no. 14, with distortion screen.

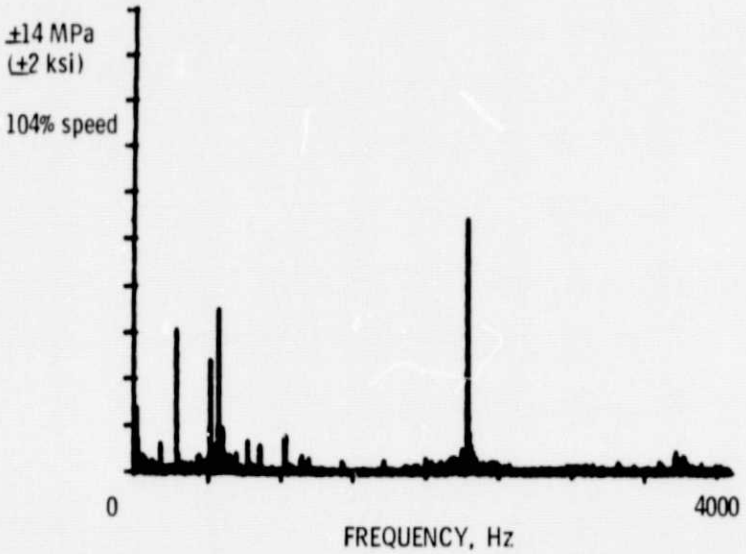

Figure 18. - Rotor 3, strain gage no. 14, with distortion screen.